

# Parameter Estimation Results of Specular and Dense Multipath Components in Micro-Cell Scenarios

A. Richter  
 Ilmenau Univ. of Technology  
 Inst. of Communications and  
 Measurement  
 98684 Ilmenau, Germany  
 ar@andyric.de

C. Schneider  
 Ilmenau Univ. of Technology  
 Inst. of Communications and  
 Measurement  
 98684 Ilmenau, Germany  
 Christian.Schneider@tu-  
 ilmenau.de

M. Landmann  
 Ilmenau Univ. of Technology  
 Inst. of Communications and  
 Measurement  
 98684 Ilmenau, Germany  
 markus.landmann@tu-  
 ilmenau.de

R. S. Thomä  
 Ilmenau Univ. of Technology  
 Inst. of Communications and  
 Measurement  
 98684 Ilmenau, Germany  
 reiner.thomae@tu-ilmenau.de

*Abstract*—Recent discussion on radio channel modelling in COST 273 has shown the importance of diffuse scattering. This paper describes the joint estimation of distributed diffuse scattered and specular components from broadband channel sounder measurements. Whereas the specular part is modelled as a finite sum of deterministic concentrated paths, the received diffuse components are represented by a stochastic process. Based upon measurements in a micro cell scenario, the relevance of this data model is shown. Both the concentrated propagation paths as well as the dense multipath components can dominate the propagation model in certain situations.

*Keywords*— Radio Channel Modelling, Channel Sounding, Radio Channel Parameter Estimation

## I. INTRODUCTION

A well accepted geometric radio channel model approximates the radio channel impulse response by a superposition of a finite number of propagation paths [1], [8]. This approach is valid for generating a realization of the radio channel, as long as the observed apertures in time, frequency and space are finite and below a certain value. The necessary input information for this channel model is a statistic model of the path parameters. The modelling accuracy can be controlled by the number of propagation paths used to generate the channel impulse response. So the synthesis problem is solved by submitting the parameter statistics of the propagation paths.

The discrete parameters and its temporal and spatial statistics can be derived from observations of the radio channel with a broadband radio channel sounder. The parameter estimates are used to derive a sufficient statistics for the radio channel propagation path parameters. This constitutes the analysis problem. Again we need a channel model to describe the observations. It has to be defined as a model, whose parameters can be estimated from the measurement data. The associated problem results from the limited amount of information about the radio channel. Because of the observations uncertainty, usually determined by the measurement noise, calibration and modelling errors the parameter estimation resolution and accuracy is limited. The minimum achievable parameter variance can be estimated using the Fisher-Information-Matrix and the Cramér-Rao-Lower bound (CRLB).

The chosen model order is said to be too complex for the available amount of information if it turns out that the lower bound on the variance of one or several model parameters is, e.g., higher than the parameter itself. Consequently we can not increase the number of propagation paths beyond this limit in order to enhance the accuracy of the radio channel model.

For this reason we have proposed in [3] to extension the data model (sum of deterministic propagation paths) for the analysis problem by an additional component describing the dense mul-

tipath components of the radio channel. This model is based on the experience from measurements that a radio channel observation has to be described by the superposition of some strong concentrated propagation paths and a large number of small propagation paths. We call the contribution of the small propagation paths as dense multipath. In this paper we discuss the relevance of the specular (concentrated) propagation paths and of the dense multipath components caused by distributed diffuse scattering in micro-cell scenarios. In the next section we provide a summary of the mathematical data model.

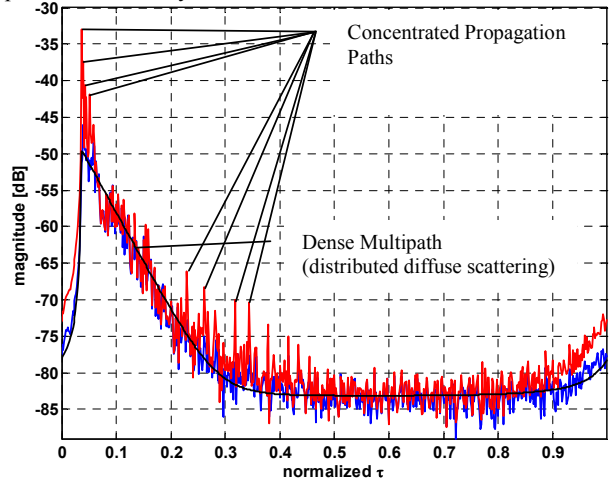


Figure 1: Measurement sequence

## II. GENERAL DATA MODEL

Let us denote a single observation of the radio channel as  $\mathbf{x}$ . Furthermore we introduce the vector valued function  $\mathbf{s}(\boldsymbol{\theta}_p)$  to express the contribution of a single propagation path to the observation in dependence of the path parameters  $\boldsymbol{\theta}_{sp}$ . There exist various ways to parameterize a propagation path, a general model is provided for example in [4]. For the dense multipath components (DMC)  $\mathbf{d}_{DMC}$  we use the model proposed in [3]. The vector  $\mathbf{d}_{DMC}$  is a circular Gaussian process with the covariance matrix  $\mathbf{R}(\boldsymbol{\theta}_{DMC})$ . Up to now all measurement data analysed so far suggest that the DMC are spatially uncorrelated, hence we assume they are correlated in the frequency domain only. Hence the covariance matrix has the structure

$$\mathbf{R}(\boldsymbol{\theta}_{DMC}) = \mathbf{I} \otimes \mathbf{R}_f(\boldsymbol{\theta}_{DMC}) \otimes \mathbf{I}.$$

The covariance matrix in the frequency domain has Toeplitz structure and is given by

$$\mathbf{R}_f(\boldsymbol{\theta}_{DMC}) = \text{toep}(\boldsymbol{\kappa}(\boldsymbol{\theta}_{DMC}), \boldsymbol{\kappa}(\boldsymbol{\theta}_{DMC})^H),$$

whereby the spectrum or better the correlation function in the frequency domain is given by

$$\boldsymbol{\kappa}(\boldsymbol{\theta}_{DMC}) = \frac{\alpha_{DMC}}{M_f} \begin{bmatrix} 1 & & \\ & \beta_{DMC} & \\ & & \dots \\ & & & \frac{e^{-j2\pi(M_f-1)\tau_{DMC}}}{\beta_d + j2\pi\frac{M_f-1}{M_f}} \end{bmatrix}^T.$$

The parameters  $\tau_{DMC}$ ,  $\alpha_{DMC}$  and  $\beta_{DMC}$  are the base time delay, the minimum attenuation and the normalized coherence bandwidth of the dense multipath components see [3] for a more detailed description of the parameters. Since every covariance matrix can be factorized into

$$\mathbf{R}(\boldsymbol{\theta}_{DMC}) = \mathbf{L}(\boldsymbol{\theta}_{DMC}) \cdot \mathbf{L}(\boldsymbol{\theta}_{DMC})^H$$

we can generate the process  $\mathbf{d}_{DMC}$  using

$$\mathbf{d}_{DMC} = \mathbf{L}(\boldsymbol{\theta}_{DMC}) \cdot \mathbf{w}_i$$

where

$$\mathbf{w}_i = \mathcal{N}(0, \frac{1}{2}\mathbf{I}) + j \cdot \mathcal{N}(0, \frac{1}{2}\mathbf{I})$$

is a multivariate i.i.d. circular Gaussian process. Altogether one channel observation can be modeled as

$$\mathbf{x} = \sqrt{\alpha_0} \cdot \mathbf{w}_0 + \mathbf{s}(\boldsymbol{\theta}_{sp}) + \mathbf{d}_{DMC}$$

whereby  $\alpha_0$  is the variance of the measurement noise.

The RIMAX algorithm described in [4] is an statistically efficient estimator for the parameters  $\boldsymbol{\theta}_{sp}$  and  $\boldsymbol{\theta}_{DMC}$ . It estimates the radio channel parameters jointly and is based on the maximum likelihood approach, it provides furthermore a mean to estimate the number of propagation paths. Using the parameter estimates one can determine an estimate of the total power of one channel observation using

$$\hat{P}_c = \mathbf{x}^H \mathbf{x} - M \cdot \hat{\alpha}_0 = \|\mathbf{x}\|_F^2 - M \cdot \hat{\alpha}_0,$$

whereby  $M$  is the length of the observation vector  $\mathbf{x}$ . Furthermore the contribution of the specular paths to the channel transfer function can be estimated using

$$\hat{P}_{sp} = \|\mathbf{s}(\hat{\boldsymbol{\theta}}_{sp})\|_F^2.$$

Finally the contribution of the dense multipath components to the given observation can be calculated using

$$\hat{P}_{DMC} = \|\mathbf{x} - \mathbf{s}(\hat{\boldsymbol{\theta}}_{sp})\|_F^2 - M \cdot \hat{\alpha}_0.$$

Using these three estimates we are able to calculate a measure of the relevance of the specular- and the dense multipath components as

$$\frac{\hat{P}_{sp}}{\hat{P}_c} \quad \text{and} \quad \frac{\hat{P}_{DMC}}{\hat{P}_c}.$$

We will use these ratios in the subsequent sections to evaluate the relevance of the DMC for a given channel.

### III. MEASUREMENT SETUP

Our channel measurements have been performed with the RUSK DoCoMo wideband channel sounder at the 5.2 GHz (WLAN band) with a bandwidth of 100 MHz. The channel sounder contains a fast multiplexing controller, which can be used to switch fast, within the coherence time of the channel, between the antenna elements of the antenna arrays throughout the channel measurement [2], [5], [6]. At the mobile transmitter an omni-directional antenna has been used, illuminating the radio channel with a transmit power of 40 dBm. At the fixed receiver, playing the role of the BS, an 8 element uniform linear array (ULA) has been used.

The channel sounder uses a strictly band-limited periodic broadband signal (multi-sinus) to excite the radio channel. The burst duration of the multi-sinus-sequence was chosen as 6.4  $\mu$ s. Since the channel sounders inserts only a blank of the same time-length to allow the antenna multiplexer and receiver to settle, all channel impulse responses between the single TX-antenna and the RX-antenna array elements can be measured in

a short time interval at one measurement point. The measurement of all 8 channel impulse responses takes 102.4  $\mu$ s. For Doppler shift resolution the measurement of the 8 channel impulse responses was repeated 4 times consecutively. The total measurement time of such a complete channel snapshot is approx. 410  $\mu$ s (see Figure 2).

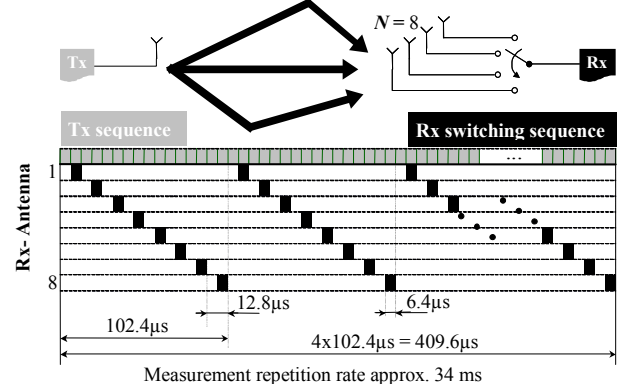


Figure 2: Measurement sequence

### IV. MEASUREMENT SCENARIO

During summer 2001 a measurement campaign has been carried out in the major street Chuo-Dori (Chuo-Avenue) downtown Tokyo, which can be characterized as typical urban with a regular street grid and high-rise buildings at both sides of the street. The street is situated in the district Nihonbashi. A measurement with a static BS position and a moving MS was conducted. Figure 2 shows a view on the scenario from the BS and Figure 3 shows a map of the measurement area.



Figure 3: Photo taken at the position of BS antenna

At the beginning of the measurement drive and at the end the LOS path could exist. In the middle part, after the car has turned off, no LOS path could exist. Altogether approx. 11000 channel observations have been recorded during the whole measurement.

### V. PARAMETER ESTIMATION RESULTS

The RIMAX algorithm described in [4], [7] has been applied to estimate the parameters  $\hat{\boldsymbol{\theta}}_{sp}$  and  $\hat{\boldsymbol{\theta}}_{DMC}$  for all channel measurements. Figure 5 shows the estimates of the three parameters  $\hat{P}_c$ ,  $\hat{P}_{sp}$  and  $\hat{P}_{DMC}$  for all observations. In Figure 6 the estimated base delay of the DMC is shown. Since the base delay is closely related to the distance between MS and BS we can use it to distinguish between sections in the measurement where the MS was moving and the section where the MS had to stop, e.g. for the traffic light. Figure 7 shows the number of propagation paths estimated by RIMAX and Figure 8 the de-

pendence of the coherence bandwidth of the DMC on their base delay, i.e. the distance between MS and BS. Figure 9 gives an overview how much power the  $p^{\text{th}}$  propagation contributes in 80%, 95% and 99% percent of the  $\sim 11000$  observations to the total power of the channel transfer function. In 99% of the cases the 30th path contributed less than 22dB to the channel transfer function. Finally Figure 10 shows the ratio between  $\hat{P}_{DMC}$  and  $\hat{P}_c$  for all observations.

To get more insight into the statistics of the parameters at first the stand still positions of the MS has been removed from the observations. In the second step the remaining data was split into two parts. The first part contains the parameters of sections 1 and 3 of the measurement drive, i.e. the sections where the LOS-path could exist (BS and MS in the same street), and the second part contains the section where the LOS-path could not exist (MS and BS not in the same street).

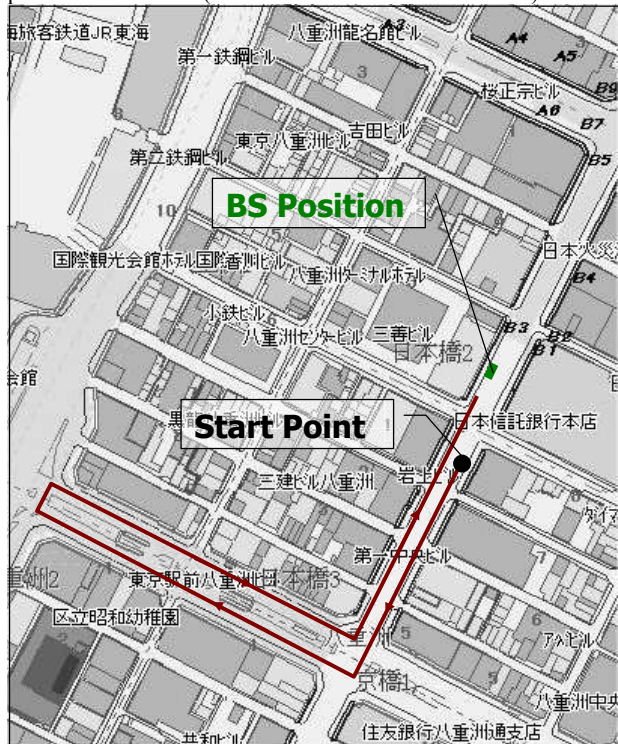


Figure 4: Map of the scenario

In Figure 11 the estimates of the three parameters  $\hat{P}_c$ ,  $\hat{P}_{sp}$  and  $\hat{P}_{DMC}$  are plotted for section 1 and 3. Here it is interesting to note, that the variation of the DMC-power is significantly smaller than the variation of the total power of the estimated specular components. In Figure 12 the ratio between  $\hat{P}_{DMC}$  and  $\hat{P}_c$  for section 1 and 3 is depicted. In average, the DMC contributes 10% to the transmission. Finally Figure 13 shows how much the  $p^{\text{th}}$  propagation path contributes in 80%, 95% and 99% percent of the  $\sim 11000$  observations to the channel transfer function in section 1 and 3. In the LOS and the NLOS cases the 25<sup>th</sup> path contributes less than -30dB to the transmission.

Whereas the specular components dominate the transmission in section 1 and 3, the DMC contributes more than 50% to the transmission in section 2. Figure 18 shows the ratio between  $\hat{P}_{DMC}$  and  $\hat{P}_c$  for this section of the estimated data. Furthermore, the variation of the total power of the specular components in the NLOS-scenario is significantly smaller than the variation of the total power of the specular components in the LOS/OLOS-scenario, see Figure 15.

It is important to note, that in section 1 and 3 the LOS was often obstructed by a car, leading to a strong variation of the total power transmitted via the specular paths. Furthermore the

contribution of the specular propagation paths to the transmission in section 1 and 3 decays clearly faster with the path number than in section 2, see Figure 13 and Figure 16. We can say the number of propagation paths necessary to model the radio channel for a scenario where both MS and BS are in the same street is significantly smaller than in a scenario where BS and MS are not in the same street. This is an important fact for channel modelling since the behaviour of the parameter estimator is quite different, it estimates more propagation paths in section 1 and 3 than in section 2, compare Figure 14 and Figure 17.

## VI. CONCLUSION

We have shown using parameter estimation results from channel sounding measurements that dense multipath components are relevant in the micro cell scenario. In non line of sight situations the DMC are the main propagation mechanism whereas in line of sight situations the specular paths clearly dominate the radio propagation between MS and BS. An observation which is also important is that the coherence bandwidth and the base delay of the DMC are strongly correlated. In the same context it is important to observe that the power of the DMC is less time variant than the total power, i.e. the power of the specular propagation paths.

## ACKNOWLEDGEMENT

The authors want to thank NTT-DoCoMo for supporting the measurement campaign and providing the measurement equipment.

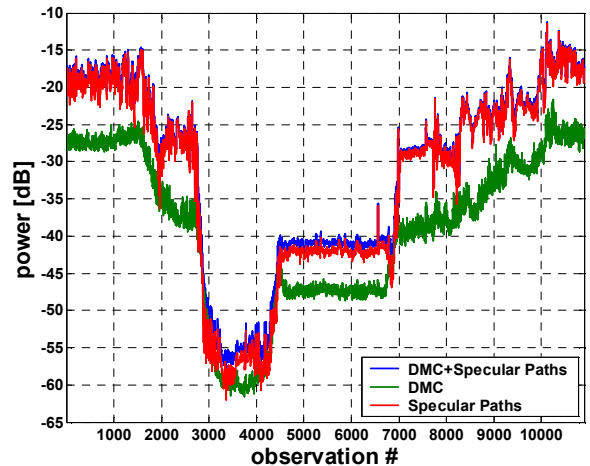


Figure 5: The parameters  $\hat{P}_c$ ,  $\hat{P}_{sp}$  and  $\hat{P}_{DMC}$  for the whole measurement drive

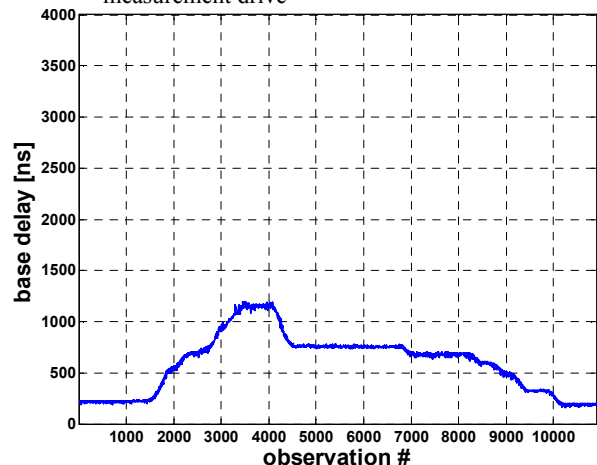


Figure 6: Estimated base delay of the DMC for the whole measurement drive

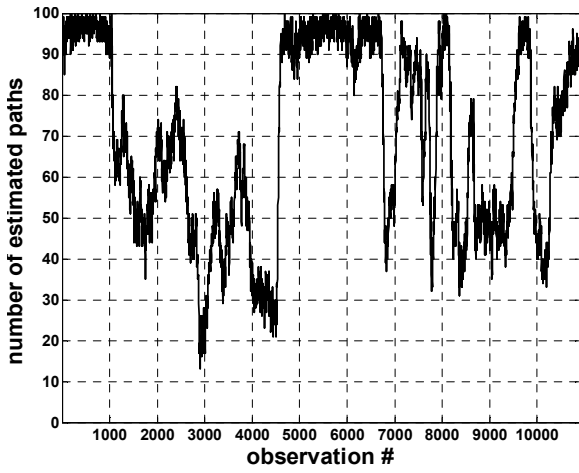


Figure 7: The number of propagation paths estimated by RIMAX (whole measurement)

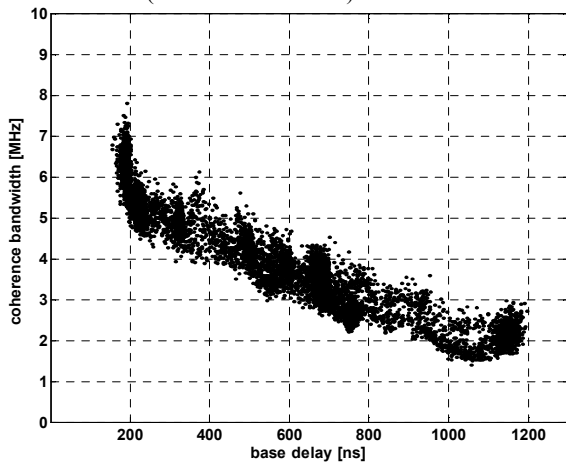


Figure 8: Dependence of the coherence bandwidth on the base delay (whole measurement)

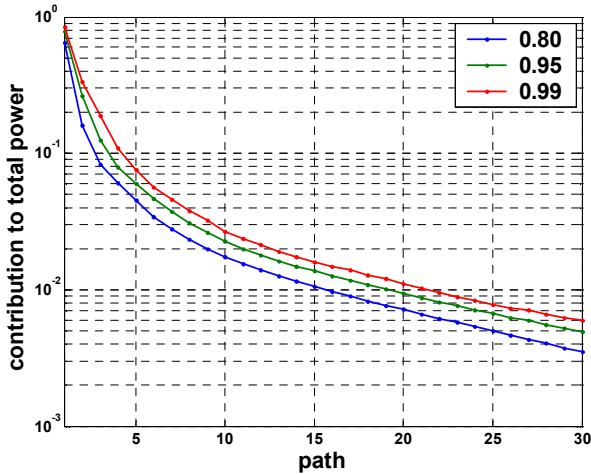


Figure 9: The contribution of the propagation paths to the channel transfer function (whole measurement)

#### REFERENCES

- [1] M. Steinbauer, "A Comprehensive Transmission and Channel Model for Directional Radio Channels," EURO-COST, TD(98)027, Bern, 2nd - 4th Feb. 1998.
- [2] R. S. Thoma, D. Hampicke, M. Landmann, G. Sommerkorn, A. Richter, "MIMO Measurement for Double-Directional Channel Modeling," Proc. IEE Technical Seminar on MIMO Communication Systems, December 12, 2001, London, UK

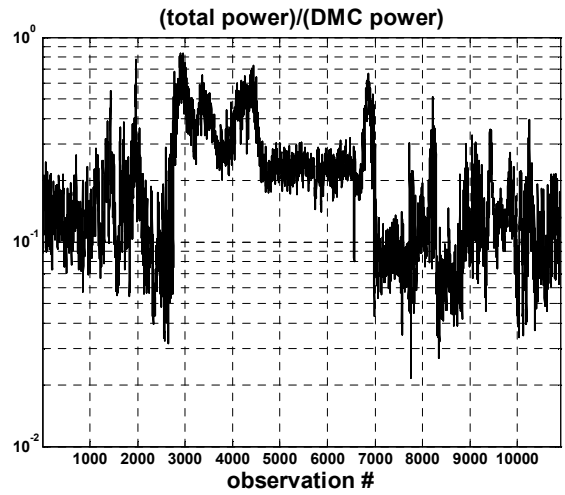


Figure 10: The ratio  $\hat{P}_{DMC}/\hat{P}_C$  for the (whole measurement) (LOS/OLOS)

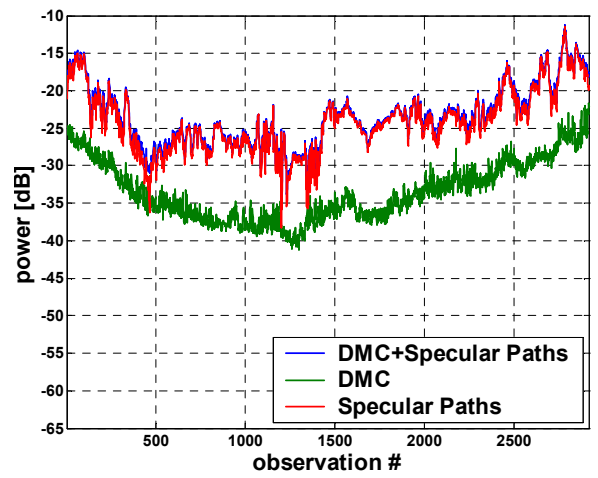


Figure 11: The parameters  $\hat{P}_c$ ,  $\hat{P}_{sp}$  and  $\hat{P}_{DMC}$  for section 1 and section 3 of the measurement (LOS/OLOS)

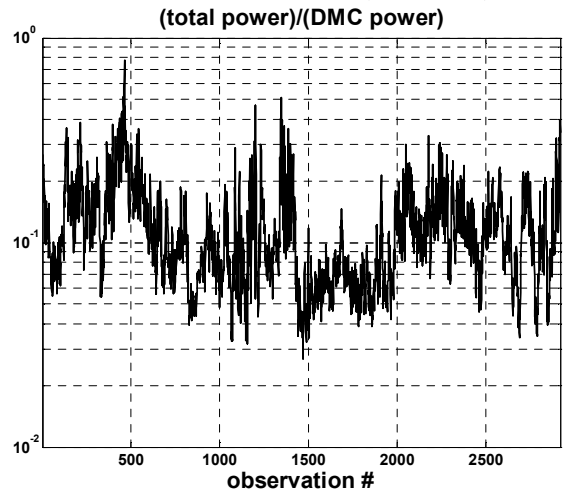


Figure 12: The ratio  $\hat{P}_{DMC}/\hat{P}_C$  for section 1 and 3 (LOS/OLOS)

- [3] Andreas Richter, Reiner S. Thoma, "Parametric Modeling and Estimation of Distributed Diffuse Scattering Components of Radio Channels", COST273, TD(03)198
- [4] Andreas Richter, Markus Landmann, Reiner S. Thoma, "RIMAX - A Flexible Algorithm for Channel Parameter Estimation from Channel Sounding Measurements", COST273, TD(04)045

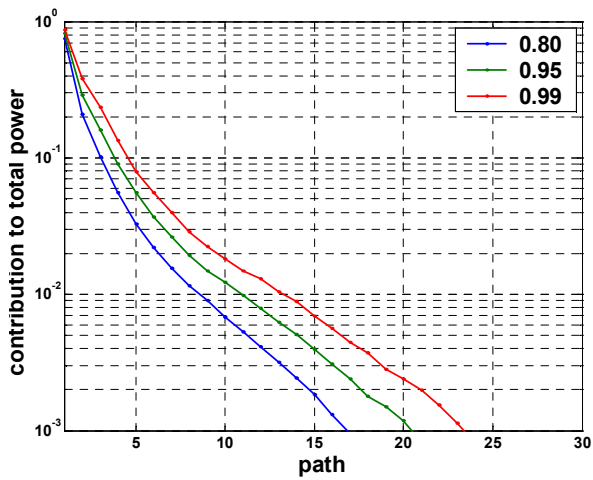


Figure 13: The contribution of the propagation paths to the channel transfer function (LOS/OLOS)

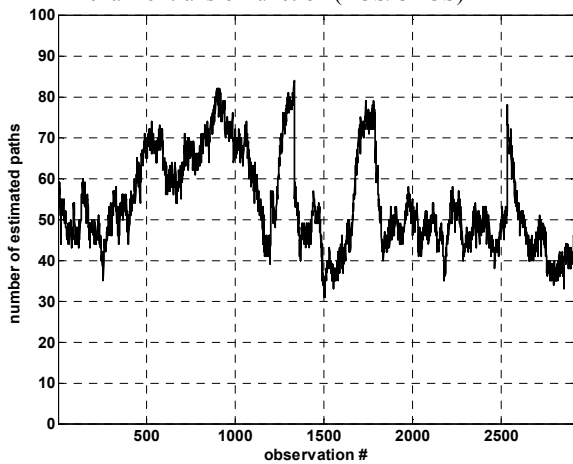


Figure 14: Number of concentrated propagation paths estimated by RIMAX in section 1 and 3 (LOS/OLOS)

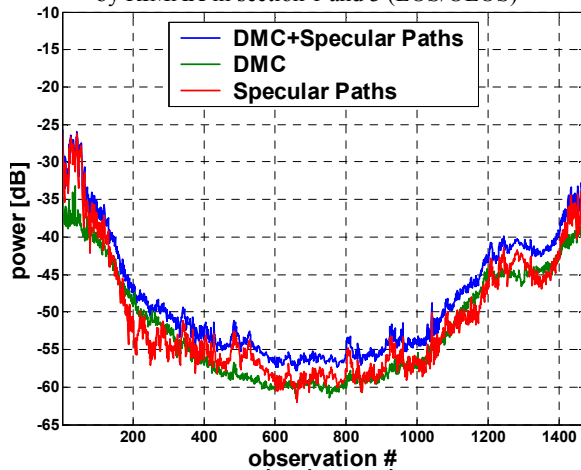


Figure 15: The parameters  $\hat{P}_c$ ,  $\hat{P}_{sp}$  and  $\hat{P}_{DMC}$  for section 2 of the measurement (NLOS)

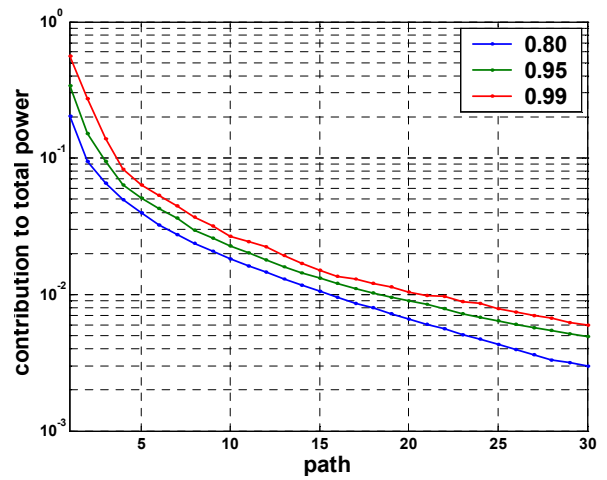


Figure 16: Contribution of the propagation paths to the channel transfer function in section 2 (NLOS)

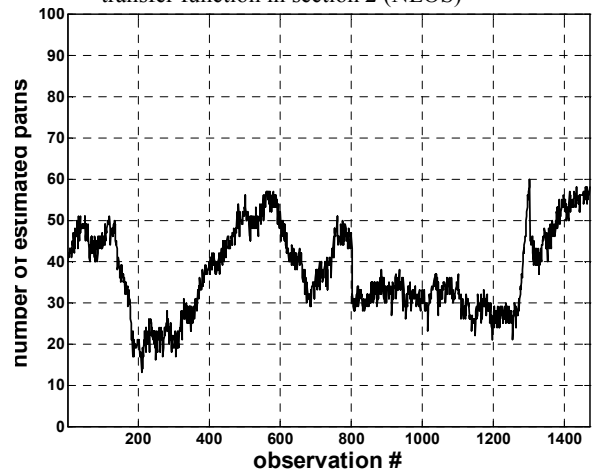


Figure 17: Number of concentrated propagation paths estimated by RIMAX in section 2 (NLOS)

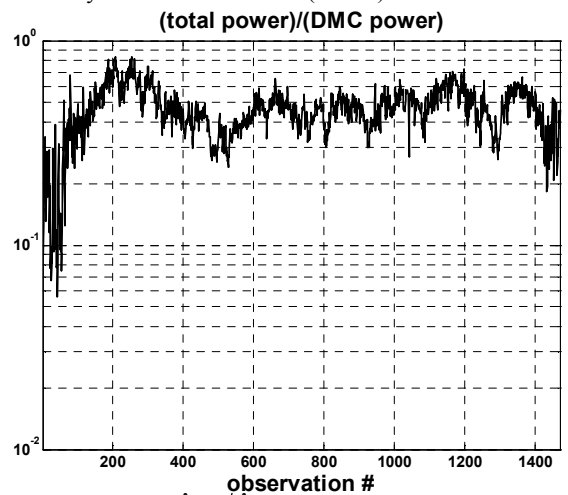


Figure 18: The ratio  $\hat{P}_{DMC}/\hat{P}_C$  for section 2 (NLOS)

[5] R.S. Thomä, D. Hampicke, A. Richter, G. Sommerkorn, U. Trautwein, "MIMO Vector Channel Sounder Measurement for Smart Antenna System Evaluation," European Transactions on Telecommunications, vol. 12, No. 5, September-October 2001

[6] Andreas Richter, Dirk Hampicke, Gerd Sommerkorn, and Reiner S. Thomae, "MIMO Measurement and Joint M-D Parameter Estimation of Mobile Radio Channels", VTC 2001-Spring, Rhodes, May 6-9, 2001

[7] A. Richter, M. Landmann, R. Thoma, "Maximum Likelihood Channel Parameter Estimation from Multidimensional Channel Sounding Measurements," IEEE VTC2003 Spring, Cheju, South Korea, April 2003

[8] A. F. Molisch, "A Generic Model for MIMO Wireless Propagation Channels in Macro- and Microcells," IEEE Trans. on Signal Processing, Vol., 52, No. 1, January 2004